



# Tau PET imaging as a mediator between glymphatic dysfunction and cognitive decline: a cross-sectional and longitudinal study

Juyeon Ko<sup>1</sup> · Gayeong Son<sup>2</sup> · Ha Eun Seo<sup>3</sup> · Jaelim Cho<sup>1</sup> · Jae-Yoon Kim<sup>2</sup> · Sang-Yoon Lee<sup>4</sup> · Daegyeom Kim<sup>3</sup> · ShinEui Park<sup>3</sup> · Kee Hyung Park<sup>5</sup> · Samuel N. Lockhart<sup>6</sup> · Dong-Hyun Kim<sup>2,7</sup> · Young Noh<sup>3,5</sup> 

Received: 30 August 2025 / Accepted: 28 December 2025  
© The Author(s) 2026

## Abstract

**Purpose** Impaired glymphatic function is considered an important characteristic of cognitive decline, but the role of tau pathology as a mediator remains unclear. This study investigated whether tau burden mediates the association between diffusion tensor image analysis along the perivascular space (DTI-ALPS) and cognitive impairment or brain atrophy. Also, we explored whether DTI-ALPS index predicts longitudinal cognitive deterioration over time.

**Methods** We included 144 individuals with mild cognitive impairment (MCI), Alzheimer's disease dementia (ADD), and other dementia, or normal cognition. All participants underwent 3.0-Tesla MRI, <sup>18</sup>F-MK6240 and <sup>18</sup>F-Flutemetamol PET scans, APOE genotyping, and comprehensive neuropsychological assessments. Among these, 101 were followed longitudinally for two years. Mediation analyses within a causal framework were used to investigate whether tau burden mediated the association between DTI-ALPS index and cognition function and structural MRI measures. Longitudinal associations were tested using linear mixed-effects models.

**Results** DTI-ALPS index was significantly lower in cognitively impaired individuals compared to cognitively normal (CN) participants. Lower DTI-ALPS index was associated with higher tau burden and worse cognitive function. Tau burden was also inversely associated with cognition. Mediation analysis indicated that tau burden accounted for approximately 21–27% of the association between DTI-ALPS and cognition. Longitudinal analysis showed baseline lower DTI-ALPS index also predicted faster longitudinal cognitive decline.

**Conclusion** Our findings suggest that the DTI-ALPS index is an indirect marker of glymphatic dysfunction associated with tau accumulation and cognitive decline. Tau pathology may partially link compromised glymphatic clearance to cognitive impairment.

**Keywords** PET · Glymphatic dysfunction · Cognitive function · Brain atrophy · Tau deposition

✉ Dong-Hyun Kim  
donghyunkim@yonsei.ac.kr

✉ Young Noh  
nymed77@gmail.com

<sup>1</sup> Department of Preventive Medicine, Yonsei University College of Medicine, Seoul, Republic of Korea

<sup>2</sup> Department of Electrical and Electronic Engineering, Yonsei University, Seoul, Republic of Korea

<sup>3</sup> Neuroscience Research Institute, Gachon University, Incheon, Republic of Korea

<sup>4</sup> Department of Neuroscience, College of Medicine, Gachon University, Incheon, Republic of Korea

<sup>5</sup> Department of Neurology, Gil Medical Center, Gachon University College of Medicine, 21, Namdong-daero, 774 beon-gil, Namdong-gu, Incheon 21565, Republic of Korea

<sup>6</sup> Perceptive, Inc, Burlington, MA, USA

<sup>7</sup> School of Electrical and Electronic Engineering, College of Engineering, Yonsei University, 50 Yonsei-ro, Seoul 03722, Republic of Korea

## Introduction

The glymphatic system is a brain-wide network that clears toxic proteins and waste products from the brain [1, 2]. Dysfunction in this system may contribute to the accumulation of amyloid beta (A $\beta$ ) plaques and hyperphosphorylated tau, which are hallmark pathologies of Alzheimer's disease dementia (ADD) [2]. The glymphatic system plays an important role in clearing A $\beta$  protein from the central nervous system, reducing its aggregation and deposition. Although tau pathology in ADD is typically intracellular, tau protein can be released extracellularly and subsequently cleared through the glymphatic system [2–4]. Thus, impaired glymphatic function could accelerate tau accumulation, leading to neurodegenerative disorders [2].

Diffusion tensor image analysis along the perivascular space (DTI-ALPS) index has emerged as a promising MRI-based biomarker for assessing glymphatic clearance efficiency [5]. The DTI-ALPS index enables glymphatic system evaluation without the need for a contrast agent. It is based on the principle that minimal perivascular water diffusion corresponds to an index close to one, with the index increasing as perivascular diffusivity increases [5]; therefore, an increasing DTI-ALPS index represents greater glymphatic flow. This technique has been used to investigate the associations between glymphatic system activity and cognitive function, and tracer uptake of amyloid imaging in patients with ADD and cognitively normal (CN) individuals [6, 7].

Although recent studies have shown that a reduced DTI-ALPS index was associated with increased tau burden (as measured by positron emission tomography [PET]) [7, 8], the causal relationship between impaired glymphatic clearance and neurodegeneration through tau deposition remains unclear. Mediation analysis is positioned well to test hypotheses about mechanisms that are at work as it determines the extent to which some potential causal variable influences some outcome, through an intermediary variable (also called 'mediator').

Several mediation studies have investigated the role of the DTI-ALPS index in cognitive decline. One study showed that the ALPS index significantly mediated the associations between A $\beta$ /tau burden and cognitive dysfunction [7]. Another found that the association between the ALPS index and cognitive decline was fully mediated by amyloid PET and brain atrophy [8]. However, these studies primarily emphasized amyloid-related pathways and structural degeneration [7, 8], without directly examining tau burden as an explicit mediator in the link between glymphatic dysfunction and cognitive outcomes. To the best of our knowledge, no previous study has investigated the mediating role of tau pathology in the association between glymphatic dysfunction and cognitive decline. Furthermore,

it remains unknown whether glymphatic dysfunction predicts pathological and clinical progression when accounting for tau burden.

The first aim of this study was to investigate whether tau burden mediates the associations of the DTI-ALPS index with both cognitive function and brain atrophy in individuals across the clinical spectrum of dementia. The second aim was to investigate the longitudinal associations between the DTI-ALPS index and changes in cognitive function over time.

## Methods

### Study participants

Participants were recruited as part of a prospective, longitudinal cohort study conducted at the memory disorder clinics within the Department of Neurology at a tertiary-care academic hospital, with a planned two-year follow-up period. Individuals with cognitive impairment (i.e., mild cognitive impairment or dementia) were enrolled through these neurology-based clinics. Cognitively normal (CN) control participants were community-dwelling volunteers recruited for aging-related research. A total of 154 individuals with MCI, ADD, other dementia, and normal cognition were enrolled. These participants underwent 3.0-Tesla MRI including DTI, <sup>18</sup>F-MK6240 (MK6240) and <sup>18</sup>F-flutemetamol (FLUTE) PET scans, APOE genotyping, and a comprehensive neuropsychological test battery at Gachon University Gil Medical Center. Both cognitive function tests and brain MRI scans were performed at baseline. Cognitive function was assessed at baseline and at one- and two-year follow-up assessments, and both cross-sectional and longitudinal cognitive data were included in the present study. Out of the 154 participants who had completed this study, a total of 10 participants were excluded: 9 due to motion artifacts on PET and 1 due to incomplete neuropsychological test results. Cross-sectional (baseline) analysis included 144 individuals (54 individuals with MCI, 38 individuals with ADD, 13 individuals with dementia other than ADD, and 39 CN individuals). Of the 144 participants, 118 individuals were scheduled to undergo follow-up cognitive function test at both the first- and second-year follow-up; 17 were lost to follow-up during the two-year period. Thus, a total of 101 participants were included in the longitudinal analyses, which consisted of 28 individuals with MCI, 41 individuals with ADD, 9 individuals with dementia other than ADD, and 23 CN individuals.

Individuals with MCI were diagnosed followed Petersen's criteria [9], requiring objective cognitive impairment (Clinical Dementia Rating–Sum of Boxes [CDR-SOB] score

= 0.5) and preserved functional independence. Individuals with ADD were identified using the NINCDS–ADRDA criteria [10]. Individuals with structural brain abnormalities on MRI—such as cerebral, cerebellar, or brainstem infarction, intracranial hemorrhage, hydrocephalus, severe white matter hyperintensities, white matter hyperintensities associated with radiation, traumatic brain injury, tumors, multiple sclerosis, and vasculitis—were excluded, as were those with secondary cognitive impairment due to metabolic or nutritional causes based on lab testing. Individuals classified as having other dementia included those clinically diagnosed with probable AD but showing negative results on amyloid PET ( $n = 8$ ), subcortical vascular dementia ( $n = 2$ ), behavioral variant frontotemporal dementia ( $n = 2$ ), and nonfluent variant primary progressive aphasia ( $n = 1$ ) [11–13].

Cognitively normal individuals were healthy volunteers from the community who showed no cognitive impairment on neuropsychological tests ( $z$ -scores within 1.5 standard deviation [SD]) and had a Clinical Dementia Rating score of 0 [14].

All participants and their legal representatives for patients with cognitive impairment provided written informed consent. The study was approved by the Gachon University Gil Medical Center IRB (IRB No. GBIRB2018-350) and registered in the Clinical Research Information Service (CRIS: KCT0005428).

### Neuropsychological assessment

All participants received a comprehensive neuropsychological evaluation, which included the Mini-Mental State Examination (MMSE) and the CDR scale [14, 15]. The full battery covered multiple cognitive domains, including attention, language, visuospatial function, verbal and visual memory, and frontal/executive functioning [16]. Details of the specific tests administered can be found in Supplementary Text 1. These evaluations were repeated annually over a 2-year period to monitor cognitive trajectories. All assessments were conducted by a licensed clinical neuropsychologist (H.S.) with 9 years of professional experience, using the same standardized battery across participants.

### MR image acquisition and analyses

#### MR imaging acquisition

All participants underwent structural MRI scanning using a 3.0 Tesla MAGNETOM Skyra system (Siemens, Germany), equipped with a 32-channel Siemens matrix head coil. The imaging protocol included DTI, 3D T1-weighted MPRAGE sequence, Fluid-Attenuated Inversion Recovery (FLAIR),

Susceptibility-Weighted Imaging (SWI), and T2-weighted imaging.

Diffusion Tensor Imaging (DTI) were collected using following parameters: TR=8800 ms, TE=89 ms, 30 diffusion directions with  $b=1000$  s/mm<sup>2</sup> and 8 volumes with  $b=0$  s/mm<sup>2</sup>, matrix size=120×120, FOV=240 mm with 70 slices. The voxel size was 2×2×2 mm<sup>3</sup> and the scan time was 6 min and 1 s. The acquisition parameters for other MRI sequences are provided in Supplementary Text 2.

#### DTI-ALPS index calculation

The Diffusion Tensor Image Analysis Along the Perivascular Space (DTI-ALPS) method was used to evaluate glymphatic system activity [6]. Color-coded fractional anisotropy (FA) maps were generated using FSL (FMRIB Software Library), and diffusivity in the  $x$ -,  $y$ -, and  $z$ -axis directions was calculated. Regions of interest (ROIs) were placed by trained operators (G.S. and J.K.) using 3×3 pixel square mask, in areas containing projection fibers and association fibers. Since the perivascular space runs parallel to the  $x$ -axis at the level of the lateral ventricle body, the ROIs were aligned along the same  $x$ -axis when placed in the projection and association fiber areas to reflect the diffusivity of the perivascular space (Supplementary Fig. 1). The operators were blind to the clinical status and PET imaging results during the ROI placement and the intraclass correlation coefficient of the ALPS index was 0.847 ( $p < 0.001$ ).

The ALPS index was calculated to assess glymphatic system activity. This index is defined as the ratio of the mean  $x$ -axis diffusivity in the areas of projection fibers and association fibers to the mean of the  $y$ -axis diffusivity in the area of projection fibers and the  $z$ -axis diffusivity in the area of association fibers. ( $ALPS\ index = \frac{mean(Dx_{proj}, Dx_{assoc})}{mean(Dy_{proj}, Dz_{assoc})}$ ) In this study, measurements were obtained from both the left and right hemispheres, and the ALPS index was calculated for each, followed by averaging to produce a single value for each participant.

#### MR imaging quantification

Structural MRI processing and volumetric measurements were performed using FreeSurfer 6.0 ([www.surfer.nmr.mgh.harvard.edu](http://www.surfer.nmr.mgh.harvard.edu)). The standard recon-all processing pipeline was applied to 3D-T1 MPRAGE images for cortical surface reconstruction and volumetric segmentation. Mean cortical thickness was calculated by averaging vertex-wise cortical thickness across bilateral hemispheres. Intracranial volume (ICV) and hippocampal volume (HV) were automatically derived using the aseg (automated segmentation) output.

All segmentations were visually inspected for accuracy and manual corrections were performed when necessary in accordance with FreeSurfer guidelines [17].

Assessment of white matter hyperintensity volume, microbleeds and lacunes are described in the Supplementary Text 3.

## PET imaging acquisition and analyses

### PET imaging acquisition

All participants underwent PET imaging with both  $^{18}\text{F}$ -MK6240 and  $^{18}\text{F}$ -FLUTE PET scans using a Siemens Biograph 6 TruePoint PET/computed tomography (CT) scanner (Siemens, Knoxville, TN, USA), employing list-mode data acquisition with 4 five-minute frames. MK6240 scans were acquired from 70 to 90 min after the intravenous injection of approximately 185 MBq of  $^{18}\text{F}$ -MK6240, which was prepared as described previously<sup>19</sup> with a modified method at the cyclotron facility of Gachon University Neuroscience Research Institute. Similarly,  $^{18}\text{F}$ -FLUTE PET scans were acquired from 90 to 110 min after the intravenous injection of 185 MBq of  $^{18}\text{F}$ -FLUTE (purchased from Carecamp Incorporated). To correct for photon attenuation, we used a low-dose CT scan. PET data was reconstructed into a  $256 \times 256 \times 109$  matrix with voxel dimensions of  $1.3 \times 1.3 \times 1.5$  mm<sup>3</sup>, using a 2D ordered subset expectation maximization algorithm with 8 iterations and 16 subsets.

The interval between  $^{18}\text{F}$ -MK-6240 PET and MRI was  $2.10 \pm 2.22$  weeks, and the interval between FLUTE PET and MRI was  $8.31 \pm 31.56$  weeks. We included six patients with Alzheimer's disease dementia who showed amyloid positivity on FLUTE PET before study enrollment. All of them performed FLUTE PET with the same protocols.

### PET quantification

For each subject, both  $^{18}\text{F}$ -MK6240 and  $^{18}\text{F}$ -FLUTE PET scans were co-registered to their corresponding T1-weighted MPRAGE MRI using FreeSurfer. Following this, we calculated regional mean uptake values after applying region-based partial volume correction (PVC) via the PETSURFER tool in FreeSurfer [18, 19] acquired weight-averaged values of pre-defined ROIs. ROIs were generated by combining the regions from the Desikan-Killiany atlas [17].

Tau burden was quantified using MK6240 SUVR. ROIs for MK-6240 included global MK6240 (Frontal pole, pars orbitalis, lateral orbitofrontal, pars triangularis, pars opercularis, rostral middle frontal, superior frontal, caudal middle frontal, medial orbitofrontal, superior parietal, inferior parietal, supramarginal, precuneus, cuneus, pericalcarine, lateral occipital, banks of superior temporal, inferior

temporal, middle temporal, superior temporal, hippocampus, amygdala, parahippocampal, entorhinal, accumbens, caudal anterior cingulate, rostral anterior cingulate and posterior cingulate), brain regions corresponding to Braak I-II (entorhinal and hippocampus regions), Braak III-IV (parahippocampal, fusiform, lingual, amygdala, inferior temporal, middle temporal, temporal pole, thalamus, caudal cingulate, rostral cingulate, isthmus cingulate, posterior cingulate and insula regions), Braak V-VI (frontal, parietal, occipital, transverse temporal, superior temporal, precuneus, banks of superior temporal, nucleus accumbens, caudate nucleus, putamen, precentral, postcentral, paracentral, cuneus and pericalcarine regions) [20, 21], and temporal meta-ROI (entorhinal cortex, amygdala, hippocampus, inferior/middle/superior temporal gyri, fusiform gyrus, and parahippocampal gyrus) [22]. Regional SUVR of MK6240 were computed using cerebellar gray matter as a reference region [23].

For amyloid PET, the cortical retention ratio of FLUTE was calculated based on AD-associated regions such as the prefrontal, superior parietal, lateral temporal, inferior parietal, occipital, anterior cingulate, mesial temporal, precuneus, and posterior cingulate cortices [24]. FLUTE SUVR was evaluated using the pons as a reference region [24]. FLUTE images were also visually evaluated for amyloid positivity based on a standardized visual rating protocol [25].

### Biological status definition of A/T/N

Individuals were classified into different amyloid (A) statuses based on  $^{18}\text{F}$ -FLUTE PET scans. Amyloid positivity was determined based on a standardized visual rating protocol. Tau positivity (T+) was determined using  $^{18}\text{F}$ -MK6240 scan, with a temporal meta-ROI SUVR  $\geq 1.35$  indicating T+ status [22]. Neurodegeneration (N+) was defined as a HV to ICV ratio ( $\text{HV}/\text{ICV} \times 1000$ ) less than 2.15 [26].

### Statistical analysis

Descriptive statistics were presented as means (SD), medians (Interquartile range), or frequencies (%). Comparisons of clinical and neuroimaging characteristics across diagnostic groups were conducted using one-way analysis of variance with Bonferroni correction ( $p < 0.05$ ). Categorical variables were compared using the chi-square test. Post-hoc analyses were conducted using Tukey's test for continuous variables and pairwise chi-square tests for categorical variables. The tau PET SUVR values for Braak I-II, III-IV, and V-VI SUVRs and hippocampus/intracranial volumes (HV/ICV) ratio were log-transformed to normalize their distribution. Sex was reported as assigned at birth, in accordance

with clinical chart records. APOE (apolipoprotein) e4 carrier status was defined as a binary variable, classified as positive if the individual carried at least one APOE e4 allele, and negative if no APOE e4 alleles were present.

Group differences in the DTI-ALPS index across diagnostic categories and A/T/N statuses (positive vs. negative) were assessed using analysis of covariance, adjusting for age, sex, educational years, and APOE e4 carrier status. Sensitivity analyses were conducted with and without individuals with other dementia.

Voxel-wise analyses were conducted to examine whole-brain associations between  $^{18}\text{F}$ -MK6240 or  $^{18}\text{F}$ -Flutemetamol SUVRs and the DTI-ALPS index. Individual PET SUVR images were spatially normalized to MNI space. Voxel-wise general linear models were applied to examine the association between PET SUVR values and subject-level DTI-ALPS indices, which were used as continuous independent variables.

To address the first aim, we first performed linear regression analyses to investigate the associations of the DTI-ALPS index (exposure) with tau burden (mediator), cognitive performance, and neurodegeneration (outcomes). Tau burden was assessed using global MK6240 SUVR, temporal meta-ROI SUVR, and regional SUVRs for Braak I–II, III–IV, and V–VI; each of these was analyzed separately in the statistical models. Cognitive function was assessed using MMSE and CDR-SOB scores, and subtests representing specific cognitive domains (attention, language, visuospatial function, memory, frontal/executive functions). Neurodegeneration markers included mean cortical thickness and hippocampal volume. All models were adjusted for age, sex, educational years, APOE e4 carrier status, and cortical FLUTE SUVR. In models involving domain-specific cognitive subtests, age, sex, and educational years were not included as covariates because the scores were z-scores adjusted for these variables. In addition, ICV was included as an additional covariate in models analyzing neurodegeneration markers (mean cortical thickness and HV/ICV ratio). The strength of association was expressed as  $\beta$ -coefficients (per unit increase in DTI-ALPS index) with corresponding standard error (SE) and p-value. Subsequently, to explore whether tau burden mediates the association between DTI-ALPS index and cognitive function (MMSE score, CDR-SOB score, and specific domains of cognitive function) and neurodegeneration markers (mean cortical thickness and HV/ICV ratio), mediation analyses were conducted using partial least squares structural equation modelling (PLS-SEM). PLS-SEM was advantageous as it does not require normality assumptions and allows for latent variable modelling through reflective measurement

structures. Among specific domains of cognitive function tested, attention, memory, and frontal/executive functions were tested as latent variables using reflective measurement models (Supplementary Fig. 2). These domains were treated as reflective measurement models because of the weak-to-moderate correlations (Pearson's correlation coefficients ranging from 0.35 to 0.64, all statistically significant) among their corresponding subtests, which supported a latent-variable approach rather than evaluating each subtest independently. To validate the PLS-SEM models, we evaluated reflective measurement models by confirming the standardized indicators and suggested cut-off values from previous studies (Supplementary Table 3). To account for correlations and directional relationships among mediators and outcomes, separate PLS-SEM analyses were conducted for each tau burden (mediators) in relation to each cognitive function and neurodegeneration markers (outcomes). All analyses were adjusted as described earlier. Direct and indirect (specific-indirect) effects were estimated by evaluating the path coefficient and 95% confidence interval with a 5,000-sample bootstrapping procedure.

To investigate the second study aim, we conducted longitudinal analyses (using a linear mixed-effects model) to investigate the association between DTI-ALPS index (measured at baseline) and changes in cognitive function (MMSE and the CDR-SOB scores). The linear mixed-effects model enabled us to simultaneously consider both within-individual and between-individual variations in cognitive function. To control for irregular time intervals between baseline and follow-up cognitive function tests (MMSE and CDR-SOB scores), the time (baseline and follow-up visits) was included in the linear mixed-effects model. Study participants were considered as a random effect. DTI-ALPS index was entered as a fixed-effect exposure variable of interest. Baseline fixed-effect covariates included age, sex, educational years, APOE e4 carrier status, and tau burden (global MK6240 retention). The strength of the association was expressed as a  $\beta$ -coefficient with a corresponding standard error (SE), and p-value.

All statistical analyses were performed using SAS software version 9.4 (SAS Institute, Cary, NC, USA), SPSS version 19 (SPSS Inc., Illinois, USA) and figures were generated in R statistical software version 4.2.2 (R Foundation for statistical computing, Vienna, Austria). PLS-SEM analysis was performed using SmartPLS (version 4). Voxel-wise analyses were performed using Statistical Parametric Mapping (SPM12; Wellcome Trust Centre for Neuroimaging, London, UK) implemented in MATLAB (R2016b; The MathWorks Inc., Natick, MA, USA). Two-sided P-values below 0.05 were considered statistically significant.

## Results

### Demographics and clinical characteristics

A total of 144 individuals were included. Mean ages did not differ across groups. Mean cortical FLUTE SUVR was significantly higher in individuals with ADD ( $0.89 \pm 0.15$ ) compared with individuals with MCI, other dementia, and CN individuals ( $p < 0.001$ ). Global MK6240 SUVR was significantly higher in individuals with ADD ( $2.65 \pm 1.39$ ) compared with individuals with MCI, other dementia, and CN individuals ( $p < 0.001$ ). Individuals with ADD had the lowest mean cortical thickness ( $2.31 \pm 0.12$  mm;  $p < 0.001$ ). Other characteristics are presented in Table 1 and Supplementary Table 1.

### Comparison of DTI-ALPS index among different diagnostic and biological groups

The mean DTI-ALPS index was the highest in individuals with CN compared with MCI, ADD, or other dementia. Group differences were statistically significant in both the unadjusted and fully-adjusted models ( $p < 0.001$  for all models). Post-hoc analyses showed that CN individuals had significantly higher DTI-ALPS index than individuals with MCI, ADD, and other dementia ( $p < 0.001$ ; Fig. 1A).

We further investigated differences in DTI-ALPS index across A/T/N biomarker statuses (positive vs. negative; Fig. 1B-D). DTI-ALPS index differed by T and N status after covariate adjustment. Individuals with T+status had lower DTI-ALPS index than those with T- status ( $1.24 \pm 0.16$  vs.  $1.31 \pm 0.23$ ;  $p = 0.028$ ), and individuals with N+status showed lower values compared with those with N- status ( $1.20 \pm 0.14$  vs.  $1.35 \pm 0.22$ ;  $p < 0.001$ ). No significant difference was found between A+ and A- ( $p = 0.156$ ).

Among individuals without other dementia, similar patterns were found for T/N statuses (Supplementary Fig. 3). Individuals with T+status showed lower DTI-ALPS index values compared with T- status ( $1.23 \pm 0.15$  vs.  $1.33 \pm 0.23$ ;  $p = 0.001$ ), and individuals with N+status also showed significantly lower values compared with N- status ( $1.18 \pm 0.13$  vs.  $1.36 \pm 0.21$ ;  $p < 0.001$ ). However, individuals with A+status had significantly lower DTI-ALPS index values than those with A- status ( $1.24 \pm 0.15$  vs.  $1.33 \pm 0.25$ ;  $p = 0.017$ ).

### Association of DTI-ALPS index with cognitive function, neurodegeneration markers, and tau burden

The associations between DTI-ALPS index and cognitive function (MMSE and CDR-SOB scores, subtests of specific

cognitive functions—except for Digit span forward and backward, RCFT copy, and Trail Making Test B) and neurodegeneration markers (mean cortical thickness and hippocampal volume) were all statistically significant ( $p < 0.05$ ; Table 2). DTI-ALPS index was negatively associated with global MK6240 SUVR ( $\beta = -1.24$ ;  $SE = 0.39$ ;  $p = 0.002$ ), Braak III-IV ( $\beta = -0.52$ ;  $SE = 0.19$ ;  $p = 0.005$ ) and Braak V-VI SUVRs ( $\beta = -0.51$ ;  $SE = 0.76$ ;  $p = 0.005$ ), and temporal meta-ROI SUVR ( $\beta = -1.57$ ;  $SE = 0.49$ ;  $p = 0.002$ ). By contrast, no significant association was found between DTI-ALPS index and Braak I-II SUVR (Table 2). Voxel-wise analysis showed that a lower DTI-ALPS index was significantly associated with increased  $^{18}\text{F}$ -MK6240 retention in widespread cortical regions (Fig. 2). These associations were significantly observed in the parietal, lateral temporal, precuneus, posterior cingulate cortex, and small areas of frontal cortex. When the same analysis was performed excluding individuals with other dementia, the regions showing increased MK6240 retention with lower DTI-ALPS exhibited a similar topography to that observed in the analysis of all subjects, with slightly more extensive involvement in the frontal, temporal, and parietal cortices (Supplementary Fig. 4).

### Mediating effects of Tau burden on associations between DTI-ALPS index and cognitive function

Global MK6240 SUVR was significantly associated with global cognition, including MMSE and CDR-SOB scores and attention, frontal/executive functions, language, memory, and visuospatial function (Table 3 and Supplementary Table 2).

Global MK6240 SUVR significantly mediated the association between DTI-ALPS index and MMSE score ( $\beta = 0.09$ ;  $SE = 0.03$ ;  $p = 0.006$ ); the proportion mediated was 27.08% (Table 3; Fig. 3A). The mediation effect of global MK6240 SUVR on the association between DTI-ALPS index and CDR-SOB score was statistically significant ( $\beta = -0.08$ ;  $SE = 0.03$ ;  $p = 0.017$ ); the proportion mediated was 21.65% (Table 3; Fig. 3B). Regarding specific cognitive function domains, the mediation effect of global MK6240 SUVR on the associations between DTI-ALPS index and frontal/executive functions ( $\beta = 0.09$ ;  $SE = 0.03$ ;  $p = 0.006$ ), language ( $\beta = 0.08$ ;  $SE = 0.03$ ;  $p = 0.013$ ), memory ( $\beta = 0.05$ ;  $SE = 0.02$ ;  $p = 0.005$ ), and visuospatial function ( $\beta = 0.03$ ;  $SE = 0.05$ ;  $p = 0.004$ ) were statistically significant (Supplementary Table 2). No significant mediation effects were observed for the attention domain.

Similar to global MK6240 retention, MK6240 retention in the brain regions for Braak III-IV, V-VI, and the temporal meta-ROI SUVRs significantly mediated the association between DTI-ALPS index and cognitive function

**Table 1** Baseline characteristics of participants included in the study

Characteristics	CN ( <i>n</i> =39)		MCI ( <i>n</i> =54)		ADD ( <i>n</i> =38)		Other dementia ( <i>n</i> =13)		<i>p</i> -value*
Age (years), mean (SD)	72.1	(5.73)	72.5	(6.62)	68.9	(10.1)	69.1	(10.3)	0.117
Male, <i>N</i> (%)	10	(25.6)	18	(33.3)	24.0	(63.2)	7.0	(53.9)	0.530
Education levels (years), mean (SD)	9.53	(4.14)	8.93	(4.92)	9.3	(4.1)	11.4	(5.22)	0.371
APOE e4 carrier status, <i>N</i> (%)	8	(20.5) <sup>b,c</sup>	32	(59.3) <sup>a,d</sup>	19.0	(50.0) <sup>a,d</sup>	2.0	(15.4) <sup>b,c</sup>	<0.001
Vascular risk factors, <i>N</i> (%)									
Hypertension	22	(56.4) <sup>c</sup>	23	(42.6)	11.0	(29.0) <sup>a</sup>	4.0	(30.8)	0.083
Diabetes mellitus	9	(23.1)	19	(35.2) <sup>c</sup>	4.0	(10.5) <sup>b</sup>	2.0	(15.4)	0.044
Dyslipidemia	20	(51.3) <sup>c</sup>	26	(48.2) <sup>c</sup>	8.0	(21.1) <sup>a,b</sup>	4.0	(30.8)	0.022
Coronary artery disease	3	(7.69)	5	(9.26)	3.0	(7.9)	0.0	(0.0)	0.734
Ischemic stroke	2	(5.13)	1	(1.85)	1.0	(2.6)	0.0	(0.0)	0.719
Cognitive function									
MMSE, mean (SD)	28.1	(1.72) <sup>b,c,d</sup>	24.8	(3.11) <sup>a,c,d</sup>	19.5	(3.61) <sup>a,b</sup>	20.6	(3.69) <sup>a,b</sup>	<0.001
CDR-SOB, mean (SD)	0.33	(0.42) <sup>b,c,d</sup>	2.12	(1.02) <sup>a,c,d</sup>	4.9	(1.96) <sup>a,b</sup>	4.9	(1.60) <sup>a,b</sup>	<0.001
Cortical FLUTE SUVR	0.43	(0.14) <sup>b,c</sup>	0.62	(0.22) <sup>a,c,d</sup>	0.89	(0.15) <sup>a,b,d</sup>	0.37	(0.06) <sup>b,c</sup>	<0.001
Amyloid Positivity, <i>N</i> (%)	7	(18.0) <sup>b,c</sup>	29	(53.7) <sup>a,c</sup>	38	(100.0) <sup>a,b,d</sup>	0	(0.00) <sup>c</sup>	<0.001
Tau burden									
Global MK6240, mean (SD)	0.97	(0.12) <sup>c</sup>	1.22	(0.42) <sup>c</sup>	2.65	(1.39) <sup>a,b,d</sup>	1.11	(0.50) <sup>c</sup>	<0.001
Braak I-II SUVR, median (25%–75%)	0.95	(0.76–1.13) <sup>b,c</sup>	1.73	(1.16–2.21) <sup>a,c</sup>	2.30	(1.66–3.01) <sup>a,b,d</sup>	1.06	(0.87–1.77) <sup>c</sup>	<0.001
Braak III-IV SUVR, median (25%–75%)	0.99	(0.89–1.09) <sup>b,c</sup>	1.17	(0.95–1.64) <sup>a,c</sup>	2.56	(1.77–3.42) <sup>a,b,d</sup>	0.98	(0.88–1.19) <sup>c</sup>	<0.001
Braak V-VI SUVR, median (25%–75%)	0.94	(0.82–1.03) <sup>c</sup>	0.96	(0.86–1.14) <sup>c</sup>	1.87	(1.30–3.01) <sup>a,b,d</sup>	0.84	(0.75–1.06) <sup>c</sup>	<0.001
Temporal meta-ROI SUVR, mean (SD)	1.11	(0.16) <sup>b,c</sup>	1.64	(0.66) <sup>a,c</sup>	3.43	(1.54) <sup>a,b,d</sup>	1.51	(0.89) <sup>c</sup>	<0.001
Brain atrophy									
Mean Cortical Thickness (mm), mean (SD)	2.45	(0.13) <sup>b,c,d</sup>	2.37	(0.13) <sup>a</sup>	2.31	(0.12) <sup>a</sup>	2.33	(0.13) <sup>a</sup>	<0.001
HV/ICV ratio, median (25%–75%)	2.48	(2.21–2.78) <sup>b,c,d</sup>	2.15	(1.95–2.44) <sup>a</sup>	2.05	(1.83–2.24) <sup>a</sup>	2.07	(1.90–2.24) <sup>a</sup>	<0.001
Total MB, mean (SD)	1.23	(2.25)	2.02	(8.27)	2.21	(1.13)	2.08	(12.3)	0.921
Total lacune, mean (SD)	1.82	(2.72)	1.30	(1.91)	0.84	(1.22)	1.46	(4.16)	0.358
Total WMHV (mm <sup>3</sup> ), mean (SD)	12.3	(10.0)	10.5	(8.75)	13.68	(6.97)	13.38	(20.9)	0.555
PWMH (mm <sup>3</sup> ), mean (SD)	10.0	(7.38)	8.84	(7.29)	10.71	(6.34)	11.78	(10.3)	0.523
DWMH (mm <sup>3</sup> ), mean (SD)	2.47	(4.13)	1.65	(4.43)	2.97	(2.22)	1.60	(13.0)	0.698
DTI-ALPS index	1.44	(0.23) <sup>b,c,d</sup>	1.23	(0.16) <sup>a</sup>	1.21	(0.12) <sup>a</sup>	1.16	(0.20) <sup>a</sup>	<0.001

**Abbreviation:** CN Cognitive normal, MCI Mild cognitive impairment, ADD Alzheimer's disease dementia, SD Standard deviation, APOE Apolipoprotein, SUVR Standardized uptake value ratio, MMSE Mini-mental state examination, CDR-SOB Clinical dementia rating-sum of boxes, HV Hippocampal volume, ICV Intracranial volume, MB Microbleeds, WMHV White matter hyperintensity volume, PWMH Periventricular white matter hyperintensity, DWMH Deep White Matter Hyperintensity

**Footnotes:** Data were presented as means (standard deviation), medians (interquartile range), or frequencies (%). HV/ICV ratio was multiplied by 1000. Regional SUVR of [<sup>18</sup>F]MK-6240 in the brain areas corresponding to Braak I–II, III–IV, and V–VI SUVR, and the HV/ICV ratio were log-transformed to normalize their distribution. Group comparisons were performed between the diagnosis groups with analysis of variance for continuous variables and chi-square test for categorical variables. For the DTI-ALPS index, analysis of covariance was used to compare diagnostic groups, adjusting for relevant covariates

Different superscript letters in a column indicate statistically significant difference between groups (determined using Tukey's test for continuous variables and pairwise chi-square tests for categorical variables.; *p*<0.05).

<sup>a</sup>Versus cognitive normal

<sup>b</sup>Versus mild cognitive impairment

<sup>c</sup>Versus Alzheimer's dementia disease

<sup>d</sup>Versus other dementia

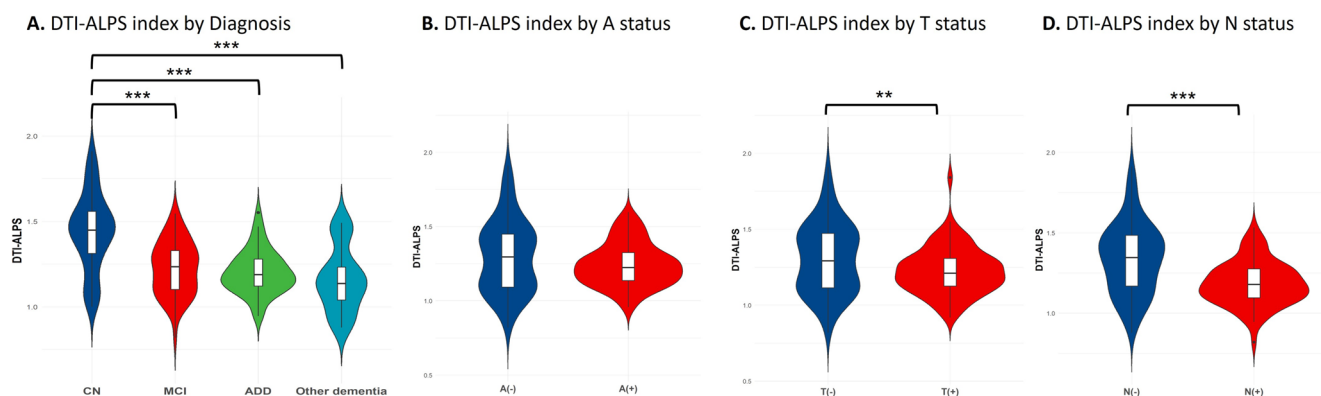


**Fig. 1** Group Comparisons of DTI-ALPS Index by Clinical Diagnosis and biological staging of all the participants. Abbreviations. CN, Cognitive normal; MCI, Mild cognitive impairment; ADD, Alzheimer's disease dementia. Footnotes. Group comparisons were conducted using analysis of covariance controlling for age, sex, educational years, and APOE e4 carrier status (A). Comparing DTI-ALPS indices in different biological groups, covariates include age, sex, educational

—including MMSE, CDR-SOB, and domain-specific measures of frontal/executive function, language, memory, and visuospatial function ( $p < 0.05$ ; Table 3; Supplementary Table 2). By contrast, MK6240 retention in Braak I–II SUVR did not significantly mediate these associations. ( $p = 0.053$  in MMSE score and  $p = 0.056$  in COR-SOB; Table 3; Supplementary Table 2).

### Mediating effects of tau burden on associations between DTI-ALPS index and neuroimaging markers

Global MK6240 SUVR was significantly associated with mean cortical thickness ( $p < 0.05$ ; Table 4). The mediation effect of global MK6240 on the association between DTI-ALPS index and mean cortical thickness was statistically significant ( $\beta = 0.07$ ;  $SE = 0.03$ ;  $p = 0.017$ ); the proportion mediated was 21.34% (Table 4; Fig. 3C). By contrast, global MK6240 SUVR was not significantly associated with HV/ICV ratio ( $p = 0.120$ ; Table 4). Consistent with this, the mediation effect was not statistically significant ( $\beta = 0.02$ ;  $SE = 0.02$ ;  $p = 0.162$ ) (Table 4; Fig. 3D).

Similar to global MK6240 retention, MK6240 retention in Braak III–IV, V–VI, and the temporal meta-ROI SUVRs significantly mediated the association between DTI-ALPS index and mean cortical thickness ( $p < 0.05$ ; Table 4). By contrast, MK6240 retention in Braak I–II SUVR did not significantly mediate these associations ( $p = 0.469$ ; Table 4). For HV/ICV ratio, MK6240 retention in Braak I–II, Braak III–IV, Braak V–VI, and the temporal meta-ROI SUVRs did not significantly mediate the association between the DTI-ALPS index and HV/ICV ratio (Table 4).

years, APOE e4 carrier, and baseline diagnoses (B–D). Amyloid positivity was defined based on a standardized visual rating protocol (B). Tau positivity was defined as a temporal meta-ROI SUVR  $\geq 1.35$  on MK6240 PET (C). Neurodegeneration positivity was defined as a Hippocampal volume/Intracranial Volume  $\times 1000 < 2.150$  (D). Significant P-values are marked with \*\* $p < 0.01$ , \*\*\* $p < 0.001$ .

### Longitudinal associations of DTI-ALPS index with changes in cognitive function

The longitudinal associations between baseline DTI-ALPS index (measured at baseline) and changes of MMSE and CDR-SOB scores over 2 years are shown in Table 5. DTI-ALPS index was positively associated with changes in MMSE score in models both without ( $\beta = 9.29$ ;  $SE = 2.00$ ;  $p < 0.001$ ) and with adjustment for global MK6240 retention ( $\beta = 5.24$ ;  $SE = 1.75$ ;  $p < 0.001$ ). DTI-ALPS index was negatively associated with changes in CDR-SOB score in models both without ( $\beta = -4.79$ ;  $SE = 1.06$ ;  $p < 0.001$ ) and with adjustment for global MK6240 retention ( $\beta = -2.97$ ;  $SE = 0.97$ ;  $p = 0.003$ ).

### Discussion

In this study, we demonstrated that lower DTI-ALPS index was significantly associated with greater tau burden, lower cognitive performance, and more severe neurodegeneration in individuals across the clinical spectrum of dementia. Using a path-analytic framework, we showed tau burden partially mediated the relationship between reduced glymphatic activity and both cognitive impairment and neurodegeneration. Specifically, tau burden (measured by Braak III–IV and V–VI SUVRs, temporal meta-ROI SUVR, and global MK6240 SUVR) partially mediated the associations between DTI-ALPS index and cognitive function (MMSE, CDR-SOB, and frontal/executive function, language, memory, and visuospatial function) and brain atrophy (mean cortical thickness), with mediation proportions ranging from

**Table 2** Associations between DTI-ALPS index and Tau burden and cognitive function tests

Independent variable	Dependent variables	$\beta$ coefficient	SE	<i>P</i> -value	
DTI_ALPS	<b>Tau burden</b>				
	Global MK6240	-1.24	0.39	0.002	
	Braak stages I-II	-0.36	0.19	0.063	
	Braak stages III-IV	-0.52	0.18	0.005	
	Braak stages V-VI	-0.52	0.76	0.005	
	Temporal meta-ROI	-1.57	0.49	0.002	
	<b>Cognitive tests</b>				
	MMSE score	8.39	1.69	<0.001	
	CDR-SOB	-4.33	0.87	<0.001	
	<b>Cognitive domains</b>				
	<i>Attention</i>				
		Digit span forward	0.39	0.41	0.338
		Digit span backward	0.42	0.44	0.347
	<i>Language function</i>				
		K-BNT	1.76	0.65	0.008
	<i>Visuospatial</i>				
		RCFT copy	2.38	1.27	0.064
	<i>Memory</i>				
		SVLT recall total	2.22	0.52	<0.001
		SVLT delayed recall	2.51	0.53	<0.001
		SVLT recognition score	3.21	0.74	<0.001
		RCFT immediate recall	1.08	0.46	0.009
		RCFT delayed recall	1.41	0.47	0.002
		RCFT recognition score	1.20	0.56	0.025
	<i>Frontal/executive functions</i>				
		COWAT animal	1.28	0.45	0.005
		COWAT supermarket	1.69	0.43	<0.001
		COWAT phonemic total score	1.33	0.45	0.003
		K-CWST	1.43	0.54	0.009
		DSC	1.77	0.61	0.004
	Trail Making Test A	0.16	2.80	0.955	
	Trail Making Test B	2.88	1.97	0.146	
<b>Neuroimaging markers</b>					
	Mean cortical thickness	0.26	0.06	<0.001	
	HV/ICV ratio	0.04	0.01	<0.001	

**Abbreviations.** DTI-ALPS Diffusion tensor image analysis along the perivascular space, *SUV*R Standardized uptake value ratio, *SNSB* Seoul neuropsychological screening battery, *MMSE* Mini-mental state examination, *SE* standard error, *CDR-SOB* clinical dementia rating–sum of boxes, *K-BNT* Korean version of the Boston naming test, *RCFT* Rey-Osterrieth complex figure test, *SVLT* Seoul verbal learning test, *COWAT* controlled oral word association test, *K-CWST* Korean-color word stroop test, *DSC* digit-symbol coding, *TMT* trail making test, *HV* Hippocampal volume, *ICV* intracranial volume

**Footnotes.**  $\beta$ -Coefficients and standard errors were estimated from multivariate generalized linear regression. All analyses were adjusted for age, sex, educational years, and APOE e4 carrier; however, age, sex, and educational years were excluded from models regressing *SNSB* tests, as *SNSB* scores were already corrected for these variables. In neuroimaging analyses, the intracranial volume was added as an additional covariate. Regional *SUV*R of 18 F-MK-6240 in the brain areas for Braak I–II, III–IV, and V–VI, and the HV/ICV ratio were log-transformed to normalize their distribution

approximately 21–27%. However, hippocampal atrophy showed no clear association with tau-mediated effects of DTI-ALPS, whereas amyloid burden appeared to play a more prominent role in hippocampal neurodegeneration. Moreover, our longitudinal analyses showed that lower baseline glymphatic function was significantly associated with faster cognitive decline over a two-year period, independent of tau burden. Even after adjusting for tau burden,

DTI-ALPS remained significantly associated with cognitive decline, indicating that this relationship may be partially mediated by tau-independent mechanisms, including neuroinflammation, synaptic dysfunction, sleep-dependent alterations in glymphatic influx, and changes in arterial pulsatility and other related pathophysiological processes.

Our results extend prior studies that used mediation analysis to examine the relationship between glymphatic

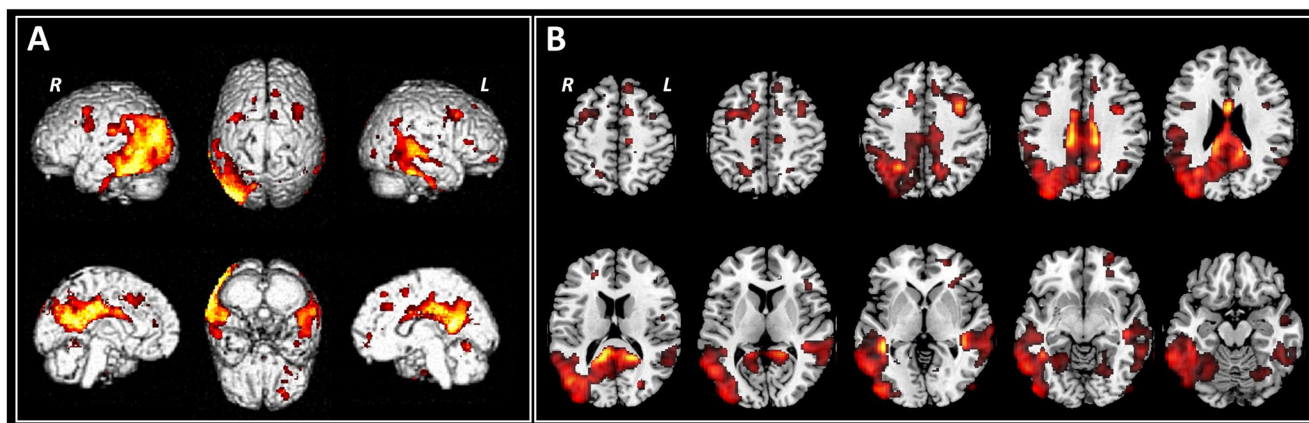


**Fig. 2** Voxel-wise associations between DTI-ALPS index and  $^{18}\text{F}$ -MK6240 retention. Footnotes. 3D surface maps (A) and 2D axial slices (B) illustrate brain regions where a lower DTI-ALPS index is significantly associated with increased  $^{18}\text{F}$ -MK6240 SUVR, indicating

higher tau burden. The statistical maps are thresholded at uncorrected  $p < 0.001$  ( $t = 3.15$ , cluster size = 0) and adjusted for age, sex, educational years, and APOE e4 carrier status

function, pathological burden, and cognition [7, 8]. While Hsu et al., focused on CN and ADD individuals, and Huang et al., included CN, MCI and ADD groups [7, 8], our study encompassed individuals across a broader range of clinical diagnoses, including other dementia types. Furthermore, unlike previous reports that emphasized amyloid pathology as a mediator, we identified tau burden—particularly in the brain areas for Braak III and above—as a key intermediary linking glymphatic dysfunction to both cognitive impairment and neurodegeneration. Notably, no association was observed in Braak I–II SUVR. One proposed mechanism for the Braak stage-dependent differences in DTI-ALPS effects lies in the heterogeneous efficiency of glymphatic clearance across brain regions. The medial temporal lobe (MTL), including the entorhinal cortex and hippocampus, may have inherently limited CSF-interstitial exchange due to its deep anatomical location and sparse perivascular pathways, whereas broad neocortical areas with extensive subarachnoid space and arterial perivascular routes experience more robust glymphatic circulation. A previous study demonstrated this disparity by showing delayed CSF clearance from the entorhinal cortex [27], indicating slow waste removal in the MTL. This localized clearance failure could accelerate tau accumulation, whereas global glymphatic decline would drive aggregation in the neocortex. In addition, tau pathology confined to the MTL at early Braak stages I–II has little clinical effect; older individuals harboring such tangles often remain cognitively normal. By contrast, once tau progresses to Braak III–IV, it is strongly associated with cognitive deficits. Therefore, early stages of tau accumulation may not be affected by glymphatic dysfunctions (shown in Tables 3 and 4). Furthermore, anatomical proximity may play a role: the medial temporal lobes affected in Braak stages I–II are located farther from the

DTI-ALPS regions of interest—projection and association fibers near the lateral ventricles—compared to neocortical regions involved in Braak stages III–VI. These regions are in closer spatial proximity to the DTI-ALPS measurement site, potentially allowing stronger detection of glymphatic impairment in association with later-stage tau deposition.

The spatial distribution of tau-glymphatic associations identified in this study differed from the frontal-predominant pattern described by Hsu et al., who described prominent tau-glymphatic associations in frontal and anterior cingulate regions. In contrast, our voxel-wise analyses demonstrated more pronounced associations in posterior cortical regions, including the parietal and lateral temporal cortices, precuneus, and posterior cingulate. Several factors may account for these discrepancies. First, differences in cohort composition and disease stage may be relevant, as Hsu et al. focused on ADD and CN individuals, whereas our cohort encompassed a broader clinical spectrum including MCI. Second, differences in participant age may partly explain the discrepant regional findings. In the study by Hsu et al., the mean age of cognitively normal (CN) participants was relatively young ( $61.0 \pm 7.1$  years), and the Alzheimer's disease dementia (ADD) group had a mean age of  $63.2 \pm 4.7$  years, suggesting that a substantial proportion of early-onset AD (EOAD) cases may have been included. In contrast, participants in our study were considerably older across all diagnostic categories, with mean ages of  $72.1 \pm 5.7$  years for CN,  $72.5 \pm 6.6$  years for MCI,  $68.9 \pm 10.1$  years for ADD, and  $69.1 \pm 10.3$  years for other dementias. Even when restricting comparisons to CN and ADD only, our cohorts were substantially older than those in Hsu et al. Moreover, within our ADD group, EOAD and late-onset AD (LOAD) were equally represented (19 EOAD and 19 LOAD). These age differences may have influenced the topographical patterns

**Table 3** Mediating effects of Tau burden on associations between DTI-ALPS index and cognitive function

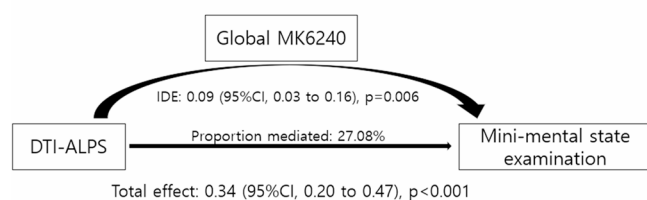
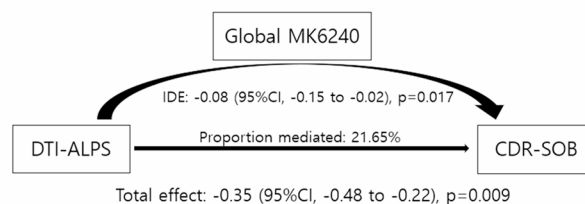
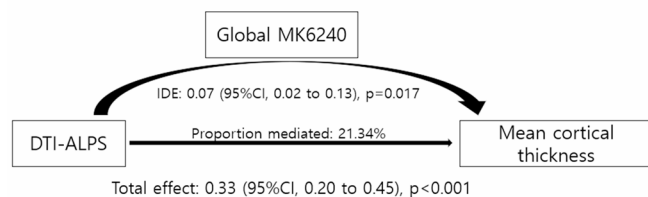
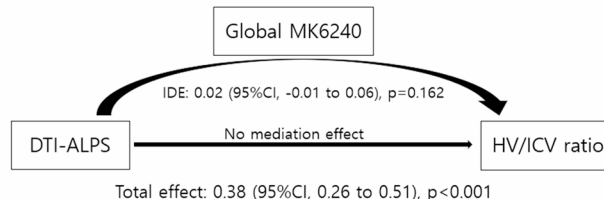
1. MMSE						
Mediators	Paths	Path coefficient	SE	t value	P-value	Decision
Global	<b>Direct effect</b>					
MK6240 SUVR	DTI-ALPS → Global MK6240	-0.19	0.06	3.32	0.001	
	DTI-ALPS → MMSE	0.34	0.07	4.86	<0.001	
	Global MK6240 → MMSE	-0.48	0.09	5.53	<0.001	
	<b>Indirect effect</b>					
	DTI-ALPS → Global MK6240 → MMSE	0.09	0.03	2.75	0.006	<i>Accepted</i>
Braak I-II	<b>Direct effect</b>					
SUVR	DTI-ALPS → Braak stages I-II	-0.17	0.08	2.15	0.031	
	DTI-ALPS → MMSE	0.37	0.07	5.61	<0.001	
	Braak stages I-II → MMSE	-0.38	0.09	4.51	<0.001	
	<b>Indirect effect</b>					
	DTI-ALPS → Braak stages I-II → MMSE	0.07	0.03	1.94	0.053	<i>Rejected</i>
Braak III-IV	<b>Direct effect</b>					
SUVR	DTI-ALPS → Braak stages III-IV	-0.20	0.07	2.93	0.003	
	DTI-ALPS → MMSE	0.36	0.07	5.25	<0.001	
	Braak stages III-IV → MMSE	-0.52	0.09	5.99	<0.001	
	<b>Indirect effect</b>					
	DTI-ALPS → Braak stages III-IV → MMSE	0.10	0.04	2.53	0.011	<i>Accepted</i>
Braak V-VI	<b>Direct effect</b>					
SUVR	DTI-ALPS → Braak stages V-VI	-0.17	0.06	2.74	0.006	
	DTI-ALPS → MMSE	0.34	0.07	4.98	<0.001	
	Braak stages V-VI → MMSE	-0.46	0.10	4.58	<0.001	
	<b>Indirect effect</b>					
	DTI-ALPS → Braak stages V-VI → MMSE		0.08	0.04	2.21	<i>Accepted</i> 0.027
Temporal meta-ROI	<b>Direct effect</b>					
SUVR	DTI-ALPS → Temporal meta-ROI	-0.21	0.06	3.32	0.001	
	DTI-ALPS → MMSE	0.35	0.07	5.09	<0.001	
	Temporal meta-ROI → MMSE	-0.51	0.08	6.31	<0.001	
	<b>Indirect effect</b>					
	DTI-ALPS → Temporal meta-ROI → MMSE	0.11	0.04	2.83	0.005	<i>Accepted</i>
2. CDR-SOB						
Mediators	Paths	Path coefficient	SE	t value	P-value	Decision
Global	<b>Direct effect</b>					
MK6240 SUVR	DTI-ALPS → Global MK6240	-0.35	0.07	5.23	<0.001	
	DTI-ALPS → CDR-SOB	-0.19	0.06	3.33	0.001	
	Global MK6240 → CDR-SOB	0.40	0.10	4.14	<0.001	
	<b>Indirect effect</b>					
	DTI-ALPS → Global MK6240 → CDR-SOB	-0.08	0.03	2.38	0.017	<i>Accepted</i>
Braak I-II	<b>Direct effect</b>					
SUVR	DTI-ALPS → Braak stages I-II	-0.39	0.07	5.91	<0.001	
	DTI-ALPS → CDR-SOB	-0.17	0.08	2.17	0.03	
	Braak stages I-II → CDR-SOB	0.41	0.08	5.00	<0.001	
	<b>Indirect effect</b>					
	DTI-ALPS → Braak stages I-II → CDR-SOB	-0.07	0.04	1.91	0.056	<i>Rejected</i>
Braak III-IV	<b>Direct effect</b>					
SUVR	DTI-ALPS → Braak stages III-IV	-0.37	0.07	5.48	<0.001	
	DTI-ALPS → CDR-SOB	-0.20	0.07	2.96	0.003	
	Braak stages III-IV → CDR-SOB	0.44	0.09	4.66	<0.001	
	<b>Indirect effect</b>					
	DTI-ALPS → Braak stages III-IV → CDR-SOB	-0.09	0.04	2.41	0.016	<i>Accepted</i>
Braak V-VI	<b>Direct effect</b>					
SUVR	DTI-ALPS → Braak stages V-VI	-0.36	0.07	5.35	<0.001	
	DTI-ALPS → CDR-SOB	-0.17	0.06	2.78	0.006	
	Braak stages V-VI → CDR-SOB	0.35	0.10	3.46	0.001	

**Table 3** (continued)

1. MMSE		Path coefficient	SE	t value	P-value	Decision
Mediators	Paths					
Global	Direct effect					
	<i>Indirect effect</i>					
	DTI-ALPS → Braak stages V-VI → CDR-SOB	-0.06	0.03	2.01	0.044	<i>Accepted</i>
Temporal meta-ROI SUVR	<i>Direct effect</i>					
	DTI-ALPS → Temporal meta-ROI	-0.36	0.07	5.36	<0.001	
	DTI-ALPS → CDR-SOB	-0.21	0.06	3.33	0.001	
	Temporal meta-ROI → CDR-SOB	0.45	0.09	5.00	<0.001	
	<i>Indirect effect</i>					
	DTI-ALPS → Temporal meta-ROI → CDR-SOB	-0.10	0.04	2.63	0.009	<i>Accepted</i>

**Abbreviations.** CDR-SOB Clinical dementia rating scale - sum of boxes, MMSE Mini-mental state examination, SE standard error, DTI-ALPS Diffusion tensor image analysis along the perivascular space, SUVR Standardized uptake value ratio

**Footnotes.** Coefficients and standard errors were estimated from partial least squares structural equation modeling with bootstrap re-sampling (5,000 iterations). All models were adjusted for age, sex, educational years, APOE e4 carrier, and cortical FLUTE SUVR. Regional SUVR of  $^{18}\text{F}$ -MK-6240 in the brain areas for Braak I–II, III–IV, and V–VI SUVRs were log-transformed to normalize their distribution

**(A) Mini-mental state examination****(B) CDR-SOB****(C) Mean cortical thickness****(D) HV/ICV ratio**

**Fig. 3** Mediating effects of global MK6240 SUVR on associations between DTI-ALPS index and MMSE score (A), CDR-SOB score (B), mean cortical thickness (C), and HV/ICV ratio (D). Abbreviations. CDR-SOB, clinical dementia rating scale - sum of boxes; CI, confidence interval; DTI-ALPS, Diffusion tensor image analysis along the perivascular space; HV/ICV ratio, hippocampal volume/intracranial volume ratio; DE, direct effect; IDE, indirect effect

of tau-glymphatic associations observed across studies. Exploratory analyses suggested stronger DTI-ALPS-tau associations in EOAD compared with LOAD, raising the possibility that the frontal predominance reported in younger cohorts may be influenced by a higher proportion of EOAD cases, whereas inclusion of MCI and LOAD may reveal broader involvement of parietal-temporal and precuneus regions (Data are not shown). Third, differences in tau PET tracers may have contributed to regional variability, given the distinct binding characteristics of  $^{18}\text{F}$ APN-1607 and  $^{18}\text{F}$ MK-6240. Lastly, analytical strategies also differed between studies: Hsu et al. adjusted for regional gray matter volume ratio when examining tau-glymphatic relationships, whereas our analyses did not include region-specific

confidence interval; DTI-ALPS, Diffusion tensor image analysis along the perivascular space; HV/ICV ratio, hippocampal volume/intracranial volume ratio; DE, direct effect; IDE, indirect effect

atrophy measures. Such adjustment may differentially affect tau-glymphatic associations across regions depending on the degree of neurodegeneration, which may partly account for differences in regional patterns between studies. Together, these cohort-related and methodological differences may underlie the divergent regional patterns observed across studies.

Another notable finding was that the DTI-ALPS index showed a stronger association with tau and neurodegeneration (T and N) than with amyloid (A) status. Individuals with T + and N + status had lower DTI-ALPS indices than their negative counterparts, whereas no significant difference was found between A + and A- groups in the total sample. This finding raised the possibility that, unlike

**Table 4** Mediating effects of Tau burden on associations between DTI-ALPS index and neuroimaging markers

1. Mean cortical thickness (Mean Cth)						
Mediators	Paths	Path coefficient	SE	t value	P-value	Decision
Global	<b>Direct effect</b>					
MK6240 SUVR	DTI-ALPS → Global MK6240	0.34	0.08	4.48	<0.001	
	DTI-ALPS → Mean CTh	-0.19	0.06	3.33	0.001	
	Global MK6240 → Mean CTh	-0.37	0.10	3.71	<0.001	
	<b>Indirect effect</b>					
	DTI-ALPS → Global MK6240 → Mean CTh	0.07	0.03	2.39	0.017	Accepted
Braak I-II	<b>Direct effect</b>					
SUVR	DTI-ALPS → Braak stages I-II	0.35	0.08	4.68	<0.001	
	DTI-ALPS → Mean CTh	-0.17	0.08	2.17	0.030	
	Braak stages I-II → Mean CTh	-0.08	0.10	0.81	0.421	
	<b>Indirect effect</b>					
	DTI-ALPS → Braak stages I-II → Mean CTh	0.01	0.02	0.72	0.469	Rejected
Braak III-IV	<b>Direct effect</b>					
SUVR	DTI-ALPS → Braak stages III-IV	0.35	0.08	4.61	<0.001	
	DTI-ALPS → Mean CTh	-0.20	0.07	2.96	0.003	
	Braak stages III-IV → Mean CTh	-0.30	0.11	2.75	0.006	
	<b>Indirect effect</b>					
	DTI-ALPS → Braak stages III-IV → Mean CTh	0.06	0.03	2.07	0.038	Accepted
Braak V-VI	<b>Direct effect</b>					
SUVR	DTI-ALPS → Braak stages V-VI	0.35	0.08	4.54	<0.001	
	DTI-ALPS → Mean CTh	-0.17	0.06	2.78	0.006	
	Braak stages V-VI → Mean CTh	-0.40	0.10	3.93	<0.001	
	<b>Indirect effect</b>					
	DTI-ALPS → Braak stages V-VI → Mean CTh	0.07	0.03	2.20	0.028	Accepted
Temporal	<b>Direct effect</b>					
meta-ROI SUVR	DTI-ALPS → Temporal meta-ROI	0.35	0.08	4.60	<0.001	
	DTI-ALPS → Mean CTh	-0.21	0.06	3.33	0.001	
	Temporal meta-ROI → Mean CTh	-0.27	0.11	2.54	0.011	
	<b>Indirect effect</b>					
	DTI-ALPS → Temporal meta-ROI → Mean CTh	0.06	0.03	2.04	0.041	Accepted
2. Hippocampal volume/intracranial volume ratio (HV/ICV ratio)						
Mediators	Paths	Path coefficient	SE	t value	P-value	Decision
Global	<b>Direct effect</b>					
MK6240 SUVR	DTI-ALPS → Global MK6240	0.38	0.06	6.00	<0.001	
	DTI-ALPS → HV/ICV ratio	-0.19	0.06	3.32	0.001	
	Global MK6240 → HV/ICV ratio	-0.13	0.08	1.56	0.120	
	<b>Indirect effect</b>					
	DTI-ALPS → Global MK6240 → HV/ICV ratio	0.02	0.02	1.40	0.162	Rejected
Braak I-II	<b>Direct effect</b>					
SUVR	DTI-ALPS → Braak stages I-II	0.41	0.07	6.23	<0.001	
	DTI-ALPS → HV/ICV ratio	-0.17	0.08	2.15	0.031	
	Braak stages I-II → HV/ICV ratio	-0.23	0.10	2.46	0.014	
	<b>Indirect effect</b>					
	DTI-ALPS → Braak stages I-II → HV/ICV ratio	0.04	0.03	1.51	0.130	Rejected
Braak III-IV	<b>Direct effect</b>					
SUVR	DTI-ALPS → Braak stages III-IV	0.39	0.06	6.17	<0.001	
	DTI-ALPS → HV/ICV ratio	-0.20	0.07	2.93	0.003	
	Braak stages III-IV → HV/ICV ratio	-0.18	0.08	2.16	0.031	
	<b>Indirect effect</b>					
	DTI-ALPS → Braak stages III-IV → HV/ICV ratio	0.04	0.02	1.77	0.077	Rejected
Braak V-VI	<b>Direct effect</b>					
SUVR	DTI-ALPS → Braak stages V-VI	0.38	0.06	6.01	<0.001	
	DTI-ALPS → HV/ICV ratio	-0.17	0.06	2.74	0.006	
	Braak stages V-VI → HV/ICV ratio	-0.13	0.09	1.49	0.137	

**Table 4** (continued)

1. Mean cortical thickness (Mean Cth)		Path coefficient	SE	t value	P-value	Decision
Global	Direct effect					
	<i>Indirect effect</i>					
	DTI-ALPS → Braak stages V-VI → HV/ICV ratio	0.02	0.02	1.27	0.205	<i>Rejected</i>
Temporal meta-ROI SUVR	<i>Direct effect</i>					
	DTI-ALPS → Temporal meta-ROI	0.39	0.06	6.06	<0.001	
	DTI-ALPS → HV/ICV ratio	-0.21	0.06	3.32	0.001	
	Temporal meta-ROI → HV/ICV ratio	-0.15	0.08	1.90	0.057	
	<i>Indirect effect</i>					
	DTI-ALPS → Temporal meta-ROI → HV/ICV ratio	0.03	0.02	1.71	0.087	<i>Rejected</i>

**Abbreviations.** *SE* standard error, *DTI-ALPS* Diffusion tensor image analysis along the perivascular space, *SUVR* Standardized uptake value ratio, *Cth* cortical thickness, *HV/ICV* ratio, hippocampal volume/intracranial volume ratio

**Footnotes.** Coefficients and standard errors were estimated from partial least squares structural equation modeling with bootstrap re-sampling (5,000 iterations). All models were adjusted for age, sex, educational years, APOE ε4 carrier, cortical FLUTE SUVR, and intracranial volume. Regional SUVR of [<sup>18</sup>F]MK-6240 in Braak I–II, III–IV, and V–VI SUVRs, and the HV/ICV ratio were log-transformed to normalize their distribution

**Table 5** Longitudinal associations of DTI-ALPS index with changes in cognitive function

Cognitive function	Model 1			Model 2		
	β	SE	p-value	β	SE	p-value
MMSE	9.29	2.00	<0.001	5.24	1.75	<0.001
CDR-SOB	-4.79	1.06	<0.001	-2.97	0.97	0.003

**Abbreviations.** *DTI-ALPS* Diffusion tensor image analysis along the perivascular space, *MMSE* Mini-mental state examination, *CDR-SOB* Clinical dementia rating-sum of boxes, *SE* standard error

**Footnotes.** Associations were assessed by linear mixed models. Model 1 was adjusted for baseline age, sex, educational years, and APOE ε4 carrier, while Model 2 additionally adjusted for global MK6240 SUVR. β-coefficients (per unit increase in DTI-ALPS index) represented estimated changes in MMSE and CDR-SOB scores

tau, Aβ may reach a ceiling effect rather than continuing to accumulate in proportion to disease severity. One possible explanation is that our study population included individuals with other dementia, in whom amyloid pathology may not be the primary pathological driver. Indeed, when individuals with other dementia were excluded, the DTI-ALPS index showed a significant difference according to A status (Supplementary Fig. 3). Alternatively, this finding aligns with the hypothesis that impaired glymphatic clearance may contribute more directly to tau accumulation and structural degeneration than to Aβ deposition alone [3, 28]. These findings highlight the importance of accounting for diagnostic heterogeneity when interpreting the relationship between glymphatic function and Aβ burden.

Taken together, these findings indicate that glymphatic dysfunction, as measured by the DTI-ALPS index, is closely associated with tau-related pathological processes. Although tau burden increased markedly from MCI to AD in our cohort, the ALPS index did not show a corresponding group-level decline. This dissociation likely reflects the timing of glymphatic impairment along the Alzheimer's disease continuum. MCI individuals already exhibited significantly lower ALPS values compared with cognitively normal participants, suggesting that glymphatic dysfunction

emerges early and reaches a relative plateau before overt dementia. Consequently, further increases in tau burden from MCI to AD may not translate into additional categorical reductions in the ALPS index. Notably, ALPS continued to show robust continuous associations with tau burden and cognitive performance, underscoring its relevance despite the lack of significant group-level differences.

From a mechanistic standpoint, these findings reinforce the role of the glymphatic system – driven by aquaporin-4 dependent fluid exchange – in tau clearance and suggest that impaired glymphatic flow may exacerbate tau-mediated neurodegeneration and cognitive decline. For example, studies using AD transgenic mice have shown that genetic deletion or pharmacological inhibition of aquaporin-4 significantly impairs the clearance of extracellular tau, leading to increased tau aggregation, accelerated spread across brain regions, and worsened cognitive deficits [4, 29]. Neuroimaging studies have further linked reduced glymphatic activity to increased amyloid and tau burden, suggesting its involvement in Alzheimer's disease pathophysiology [7]. Our study extends this mechanism by demonstrating that tau burden significantly mediated the relationship between glymphatic system (measured by the DTI-ALPS index) and neurodegeneration. Given that glymphatic function is modifiable by

sleep, vascular health, and physical activity [30–33], these results open new avenues for potential therapeutic interventions targeting clearance mechanisms in early-stage ADD.

This study has several strengths. It included a well-characterized cohort comprising individuals across the clinical spectrum of dementia and supported by multimodal biomarkers, including both tau and amyloid PET imaging. Also, the present study incorporated longitudinal follow-up and comprehensive cognitive assessments (MMSE, CDR-SOB, and detailed neuropsychological tests). The use of advanced mediation and structural equation modelling allowed us to examine potential pathways in a more structured manner, while recognizing that the cross-sectional nature of some measures limits the interpretation.

Several limitations should be acknowledged. First, the observational design limits causal interpretation. Second, although the DTI-ALPS index is a promising proxy for glymphatic function, it does not directly measure cerebrospinal fluid flow and may be influenced by other microstructural changes. It provides a global estimate and overlooks regional heterogeneity. Future studies should focus on ADD-specific regions and incorporate more sensitive biomarkers to better understand regional glymphatic function. In addition, data on circadian rhythm, sleep, and several vascular factors were not available, and therefore could not be included. Future studies with more complete covariate information are needed. Third, the present study was conducted at a single center with a modest sample size, which may limit generalizability. Because glymphatic imaging markers such as the DTI-ALPS index currently lack established normative values or standardized cutoffs, our findings should be interpreted with caution, and further multicenter standardization studies are needed. Fourth, glymphatic imaging markers such as the DTI-ALPS index lack direct pathologic validation in human dementia, and current *in vivo* imaging cannot distinguish impaired tau clearance from increased tau accumulation or production. Accordingly, the associations observed in this study reflect relationships with net tau burden rather than specific clearance mechanisms, highlighting the need for future post-mortem and multimodal validation studies. Lastly, although we adjusted for tau burden in longitudinal models, future studies incorporating repeat tau PET scans will be needed to evaluate how dynamic changes in glymphatic function and tau interact over time. In the present study, mediation analyses were based on cross-sectional data, with tau burden (as the mediator) collected at a single time point. The cognitive function tests were conducted annually, with a total of three assessments, but some of the data were incomplete. Therefore, mediation analyses were conducted cross-sectionally to maximize data availability and maintain analytical consistency. While our design does

not allow for strong causal inference, our mediation hypothesis was formulated based on previous evidences showing that glymphatic dysfunction contributes to the accumulation of pathological proteins, which in turn promote neuroinflammation and cognitive decline [3, 28, 34].

In conclusion, the present study found that the DTI-ALPS index may serve as a non-invasive biomarker for glymphatic system dysfunction in dementia. Its association with cognitive decline was partially mediated by tau pathology, and baseline DTI-ALPS index values also predicted future cognitive trajectory over two years. These findings suggest that impaired glymphatic clearance contributes to neurodegeneration by facilitating tau accumulation and support glymphatic activity as a potential therapeutic target.

**Supplementary Information** The online version contains supplementary material available at <https://doi.org/10.1007/s00259-025-07756-4>.

**Acknowledgements** This research was supported by a grant of the Korea Dementia Research Project through the Korea Dementia Research Center (KDRC), funded by the Ministry of Health & Welfare and Ministry of Science and ICT, Republic of Korea (grant number: RS-2024-00334574), a grant from the Basic Science Research Program through the National Research Foundation of Korea (NRF) that is funded by the Ministry of Education (RS-2021-NR060117), a grant from the National Research Council of Science & Technology grant supervised by the Ministry of Science and ICT (Global TOP Strategic Research Program, GTL25071-000), and a grant supported by Gachon University Gil Medical Center (Grant number: FRD2022-16 and FRD2025-01).

**Author contributions** J.K.: Formal analysis, Investigation, Writing – original draft. G.S.: Investigation, Methodology. H.S.: Data curation, Investigation. J.C.: Methodology, Writing – review & editing. J.K.: Methodology, Writing – review. S.L.: Investigation, Writing – review. D.K.: Investigation, Writing. S.P. Investigation. K.P.: Investigation. S.L.: Supervision, Writing – review. D.K.: Methodology, Supervision, Writing – review. Y.N.: Conceptualization, Methodology, Writing – review & editing, Supervision, Funding acquisition. The manuscript was written through contributions of all authors. All authors have given approval to the final version of the manuscript.

**Funding** This research was supported by a grant of the Korea Dementia Research Project through the Korea Dementia Research Center (KDRC), funded by the Ministry of Health & Welfare and Ministry of Science and ICT, Republic of Korea (grant number: RS-2024-00334574), a grant from the Basic Science Research Program through the National Research Foundation of Korea (NRF) that is funded by the Ministry of Education (RS-2021-NR060117), a grant from the National Research Council of Science & Technology grant supervised by the Ministry of Science and ICT (Global TOP Strategic Research Program, GTL25071-000), and a grant supported by Gachon University Gil Medical Center (Grant number : FRD2022-16 and FRD2025-01).

**Data availability** The datasets used and/or analyzed during the current study are available from the corresponding author on reasonable request.

## Declarations

**Ethics Declaration** The study was approved by the Gachon University Gil Medical Center IRB (IRB No. GBIRB2018-350) and registered in the Clinical Research Information Service (CRIS: KCT0005428). All procedures followed the 1964 Helsinki declaration and its later amendments or comparable ethical standards. All participants and their legal representatives for patients provided written informed consent.

**Open access** This article is licensed under a Creative Commons Attribution 4.0 International License, which permits use, sharing, adaptation, distribution and reproduction in any medium or format, as long as you give appropriate credit to the original author(s) and the source, provide a link to the Creative Commons licence, and indicate if changes were made. The images or other third party material in this article are included in the article's Creative Commons licence, unless indicated otherwise in a credit line to the material. If material is not included in the article's Creative Commons licence and your intended use is not permitted by statutory regulation or exceeds the permitted use, you will need to obtain permission directly from the copyright holder. To view a copy of this licence, visit <http://creativecommons.org/licenses/by/4.0/>.

**Competing interests** The authors report no competing interests. SNL is an employee of Perceptive, Inc.

**Open Access** This article is licensed under a Creative Commons Attribution-NonCommercial-NoDerivatives 4.0 International License, which permits any non-commercial use, sharing, distribution and reproduction in any medium or format, as long as you give appropriate credit to the original author(s) and the source, provide a link to the Creative Commons licence, and indicate if you modified the licensed material. You do not have permission under this licence to share adapted material derived from this article or parts of it. The images or other third party material in this article are included in the article's Creative Commons licence, unless indicated otherwise in a credit line to the material. If material is not included in the article's Creative Commons licence and your intended use is not permitted by statutory regulation or exceeds the permitted use, you will need to obtain permission directly from the copyright holder. To view a copy of this licence, visit <http://creativecommons.org/licenses/by-nc-nd/4.0/>.

## References

- Ilf JJ, Wang M, Liao Y, Plogg BA, Peng W, Gundersen GA, et al. A paravascular pathway facilitates CSF flow through the brain parenchyma and the clearance of interstitial solutes, including amyloid  $\beta$ . *Sci Transl Med*. 2012;4:147ra111. <https://www.science.org>.
- Nedergaard M, Goldman SA. Glymphatic failure as a final common pathway to dementia. *Science*. 2020;370:50–6. <https://doi.org/10.1126/science.abb8739>.
- Harrison IF, Ismail O, Machhada A, Colgan N, Ohene Y, Nahavandi P, et al. Impaired glymphatic function and clearance of Tau in an Alzheimer's disease model. *Brain*. 2020;143:2576–93. <https://doi.org/10.1093/brain/awaa179>.
- Ishida K, Yamada K, Nishiyama R, Hashimoto T, Nishida I, Abe Y, et al. Glymphatic system clears extracellular Tau and protects from Tau aggregation and neurodegeneration. *J Exp Med*. 2022;219:e20211275. <https://doi.org/10.1084/jem.20211275>.
- Taoka T, Naganawa S. Glymphatic imaging using MRI. *J Magn Reson Imaging*. 2020;51:11–24. <https://doi.org/10.1002/jmri.26892>.
- Steward CE, Venkatraman VK, Lui E, Malpas CB, Ellis KA, Cyarto EV, et al. Assessment of the DTI-ALPS parameter along the perivascular space in older adults at risk of dementia. *J Neuroimaging*. 2021;31:569–78. <https://doi.org/10.1111/jon.12837>.
- Hsu JL, Wei YC, Toh CH, Hsiao IT, Lin KJ, Yen TC, et al. Magnetic resonance images implicate that glymphatic alterations mediate cognitive dysfunction in Alzheimer disease. *Ann Neurol*. 2023;93:164–74. <https://doi.org/10.1002/ana.26516>.
- Huang SY, Zhang YR, Guo Y, Du J, Ren P, Wu BS, et al. Glymphatic system dysfunction predicts amyloid deposition, neurodegeneration, and clinical progression in Alzheimer's disease. *Alzheimer's Dement*. 2024;20:3251–69. <https://doi.org/10.1002/alz.13789>.
- Petersen RC. Clinical practice. Mild cognitive impairment. *N Engl J Med*. 2011;364:2227–34.
- Dubois B, Feldman HH, Jacova C, Dekosky ST, Barberger-Gateau P, Rey Cummings J, et al. Research criteria for the diagnosis of Alzheimer's disease: revising the NINCDS-ADRDA criteria. *Lancet Neurol*. 2007;6:734. <https://doi.org/10.1016/S1474>.
- Rascovsky K, Hodges JR, Knopman D, Mendez MF, Kramer JH, Neuhaus J, et al. Sensitivity of revised diagnostic criteria for the behavioural variant of frontotemporal dementia. *Brain*. 2011;134:2456–77. <https://doi.org/10.1093/brain/awr179>.
- Gorno-Tempini ML, Hillis AE, Weintraub S, Kertesz A, Mendez M, Cappa SF, et al. Classification of primary progressive aphasia and its variants. *Neurology*. 2011;76:1006–14. [www.neurology.org](http://www.neurology.org).
- Kim GH, Lee JH, Seo SW, Ye BS, Cho H, Kim HJ, et al. Seoul criteria for PiB(-) subcortical vascular dementia based on clinical and MRI variables. *Neurology*. 2014;82:1529–35. <https://doi.org/10.1212/WNL.0000000000000360>.
- Morris JC. The clinical dementia rating (CDR): current version and scoring rules. *Neurology*. 1993;43:2412–2014. <https://doi.org/10.1212/WNL.43.11.2412-a>.
- Kim J, Jahng S, Kim S, Kang Y. A comparison of item characteristics and test information between the K-MMSE~2:SV and K-MMSE. *Dement Neurocogn Disord*. 2024;23:117. <https://doi.org/10.12779/dnd.2024.23.3.117>.
- Ahn H-J, Chin J, Park A, Lee BH, Suh MK, Seo SW, et al. Seoul neuropsychological screening Battery-Dementia version (SNSB-D): A useful tool for assessing and monitoring cognitive impairments in dementia patients. *J Korean Med Sci*. 2010;25:1071. <https://doi.org/10.3346/jkms.2010.25.7.1071>.
- Desikan RS, Ségonne F, Fischl B, Quinn BT, Dickerson BC, Blacker D, et al. An automated labeling system for subdividing the human cerebral cortex on MRI scans into gyral based regions of interest. *Neuroimage*. 2006;31:968–80. <https://doi.org/10.1016/j.neuroimage.2006.01.021>.
- Greve DN, Svarer C, Fisher PM, Feng L, Hansen AE, Baare W, et al. Cortical surface-based analysis reduces bias and variance in kinetic modeling of brain PET data. *Neuroimage*. 2014;92:225–36. <https://doi.org/10.1016/j.neuroimage.2013.12.021>.
- Greve DN, Salat DH, Bowen SL, Izquierdo-Garcia D, Schultz AP, Catana C, et al. Different partial volume correction methods lead to different conclusions: an 18F-FDG-PET study of aging. *Neuroimage*. 2016;132:334–43. <https://doi.org/10.1016/j.neuroimage.2016.02.042>.
- Braak H, Alafuzoff I, Arzberger T, Kretschmar H, Del Tredici K. Staging of Alzheimer disease-associated neurofibrillary pathology using paraffin sections and immunocytochemistry. *Acta Neuropathol*. 2006;112:389–404. <https://doi.org/10.1007/s00401-006-0127-z>.
- Schöll M, Lockhart SN, Schonhaut DR, O'Neil JP, Janabi M, Ossenkoppele R, et al. PET imaging of Tau deposition in the aging human brain. *Neuron*. 2016;89:971–82. <https://doi.org/10.1016/j.neuron.2016.01.028>.

22. Leuzy A, Pascoal TA, Strandberg O, Insel P, Smith R, Mattsson-Carlgrén N, et al. A multicenter comparison of [18F]flortaucipir, [18F]RO948, and [18F]MK6240 tau PET tracers to detect a common target ROI for differential diagnosis. *Eur J Nucl Med Mol Imaging*. 2021;48:2295–305. <https://doi.org/10.1007/s00259-021-05401-4>.
23. Betthausen TJ, Cody KA, Zammit MD, Murali D, Converse AK, Barnhart TE, et al. In vivo characterization and quantification of neurofibrillary Tau PET radioligand 18F-MK-6240 in humans from alzheimer disease dementia to young controls. *J Nucl Med*. 2019;60:93–9. <https://doi.org/10.2967/jnumed.118.209650>.
24. Thurfjell L, Lilja J, Lundqvist R, Buckley C, Smith A, Vandenberghe R, et al. Automated quantification of 18F-flutemetamol PET activity for categorizing scans as negative or positive for brain amyloid: concordance with visual image reads. *J Nucl Med*. 2014;55:1623–8. <https://doi.org/10.2967/jnumed.114.142109>.
25. Salloway S, Gamez JE, Singh U, Sadowsky CH, Villena T, Sabbagh MN, et al. Performance of [18F]flutemetamol amyloid imaging against the neuritic plaque component of CERAD and the current (2012) NIA-AA recommendations for the neuropathologic diagnosis of alzheimer's disease. *Alzheimer's Dementia: Diagnosis Assess Disease Monit*. 2017;9:25–34. <https://doi.org/10.1016/j.dadm.2017.06.001>.
26. Mattsson-Carlgrén N, Leuzy A, Janelidze S, Palmqvist S, Stomrud E, Strandberg O, et al. The implications of different approaches to define AT(N) in Alzheimer disease. *Neurology*. 2020;94:e2233–44. <https://doi.org/10.1212/WNL.0000000000009485>.
27. Eide PK, Ringstad G. In vivo imaging of molecular clearance from human entorhinal cortex: a possible method for preclinical testing of dementia. *Gerontol Geriatr Med*. 2019. <https://doi.org/10.1177/2333721419889739>.
28. Lopes DM, Wells JA, Ma D, Wallis L, Park D, Llewellyn SK, et al. Glymphatic inhibition exacerbates tau propagation in an Alzheimer's disease model. *Alzheimers Res Ther*. 2024;16:71. <https://doi.org/10.1186/s13195-024-01439-2>.
29. Iliff JJ, Chen MJ, Plog BA, Zeppenfeld DM, Soltero M, Yang L, et al. Impairment of glymphatic pathway function promotes tau pathology after traumatic brain injury. *J Neurosci*. 2014;34:16180–93. <https://doi.org/10.1523/JNEUROSCI.3020-14.2014>.
30. Xie L, Kang H, Xu Q, Chen MJ, Liao Y, Thiyagarajan M, et al. Sleep drives metabolite clearance from the adult brain. *Science*. 2013;342:373–7. <https://doi.org/10.1126/science.1241224>.
31. Stuckenschneider T, Askew CD, Rüdiger S, Polidori MC, Abeln V, Vogt T, et al. Cardiorespiratory fitness and cognitive function are positively related among participants with mild and subjective cognitive impairment. *J Alzheimers Dis*. 2018;62:1865–75. <https://doi.org/10.3233/JAD-170996>.
32. He X, Liu D, Zhang Q, Liang F, Dai G, Zeng J, et al. Voluntary exercise promotes glymphatic clearance of amyloid beta and reduces the activation of astrocytes and microglia in aged mice. *Front Mol Neurosci*. 2017;10:144. <https://doi.org/10.3389/fnmol.2017.00144>.
33. von Holstein-Rathlou S, Petersen NC, Nedergaard M. Voluntary running enhances glymphatic influx in awake behaving, young mice. *Neurosci Lett*. 2018;662:253–8. <https://doi.org/10.1016/j.neulet.2017.10.035>.
34. Szlufik S, Kopeć K, Szleszkowski S, Koziorowski D. Glymphatic system pathology and neuroinflammation as two risk factors of neurodegeneration. *Cells*. 2024;13:286. <https://doi.org/10.3390/cells13030286>.

**Publisher's note** Springer Nature remains neutral with regard to jurisdictional claims in published maps and institutional affiliations.